The Iranian Journal of Mechanical Engineering Transactions of ISME
Journal homepage: https://jmee.isme.ir/
Vol. 25, No. 1, 2024, pp. 6-20

Research Paper

DOI: https://doi.org/10.30506/jmee.2024.2013679.1324

Investigating the Impact of Geometric Parameters on Radial Fan Performance

Kowsar Moradihaji[*]
M.Sc.

Majid Ghassemi[†]
Professor

Mahdi Pourbagian[‡]
Assistant Professor

This study focuses on the evaluation of the performance of a radial fan, which is an essential component of various industrial and HVAC systems. The geometric parameters of the radial fan were simulated using ANSYS Workbench software, allowing for a detailed examination of its behavior under different operating conditions. Empirical data was collected through an experimental setup, enabling a comparison with the simulation results. The findings of this study indicate a high level of agreement between the simulation and experimental results, with a maximum discrepancy of only 3%. This close alignment highlights the accuracy and reliability of the simulation model. Furthermore, a comprehensive parametric analysis was conducted, focusing on four critical parameters: the number of blades, impeller width (the distance between the disk and shroud), outlet angle, and inlet angle. Variations in these parameters were explored, paying particular attention to their impact on three key performance metrics: the total pressure difference between the inlet and outlet, the static pressure difference between the inlet and outlet, and the fan's efficiency. Additionally, the study assessed the changes in shaft power resulting from these alterations.

Keywords: Radial fan, Computational simulation, Experimental analysis, Geometric parameters, Performance evaluation, Parametric analysis

1 Introduction

Radial fans, also known as centrifugal fans, play a pivotal role in a wide range of applications, from maintaining indoor air quality in HVAC systems to facilitating industrial processes that rely on controlled airflow.

[*]M.Sc., Department of Mechanical Engineering, K. N. Toosi University of Technology, No. 7, Pardis St., Mollasadra Ave., Vanak Sq., Tehran 19919-43344, Iran, kosar.moradihaji@gmail.com
[†]Professor, Department of Mechanical Engineering, K. N. Toosi University of Technology, No. 7, Pardis St., Mollasadra Ave., Vanak Sq., Tehran 19919-43344, Iran, ghasemi@kntu.ac.ir
[‡]Corresponding Author, Assistant Professor, Computational and Data-Driven Multiphysics Laboratory, Department of Mechanical Engineering, K. N. Toosi University of Technology, No. 7, Pardis St., Mollasadra Ave., Vanak Sq., Tehran 19919-43344, Iran, pourbagian@kntu.ac.ir

Received: 2023/10/17, Revised: 2024/01/14, Accepted: 2024/03/09

These fans are recognized for their ability to generate high-pressure differences, making them indispensable in scenarios where efficient air movement is imperative. Understanding the performance of radial fans is not only essential for ensuring optimal operation but also for enhancing energy efficiency and cost-effectiveness.

Behzadmehr et al. [1] investigated the influence of logarithmic and constant deceleration blade profiles on entropy generation. They compared the results of a hyperbolic shroud to those of a shroud parallel to the backplate, and discovered that the shroud parallel to the backplate produced higher entropy. Kim et al. [2] conducted a study on the performance of radial fans and their flow behavior under various parameters to aid in the design process. The $k-\varepsilon$ turbulence model is the best model for forecasting the value of relative velocity, according to Feng et al.'s [3] study of the impact of selecting various turbulence models on output results under design and off-design situations. The experimental outcomes were also compared to the numerical solution. Gui et al. [4] proposed a method for identifying key parameters within the impeller of a radial fan. Chunxi et al. [5] examined the effect of increasing impeller size on centrifugal fan performance. They investigated three different sizes of impellers for this study and did not change the size of the volute in any of the three cases. It was discovered that increasing the size of the impeller increased total pressure. Jafarzadeh et al. [6] investigated a centrifugal pump with low and high specific speed in three dimensions and found a good match between numerical and experimental solutions. Singh et al. [7] investigated the effect of geometric characteristics of a centrifugal fan used in the automotive industry. They also performed experimental data collection to validate the simulation results. Petit et al. [8] examined centrifugal pump simulations for steady and unsteady flow. A comparison of their numerical solution findings with laboratory data revealed that, while the unsteady solution results are closer to the experimental results than the steady solution, the steady solution can attain acceptable accuracy. Ratter et al. [9] introduced a comprehensive optimization approach for radial fans lacking housing, aiming to enhance their efficiency. They proposed a unique algorithm that utilizes CFD calculations to adjust the leading and trailing edges of the fan blades. Sun et al. [10] proposed a new cross flow fan design based on experimental and two-dimensional numerical results. The effectiveness of the fan was improved, and vortex shedding was reduced, with their new design. Rajabi et al [11] chose some blade parameters of axial fan and investigated the effect of those parameters on fan performance. Huang et al. [12] used the open-source OpenFOAM code to investigate the experimental and simulation findings of a centrifugal pump. The results revealed a strong correlation between numerical and experimental analysis. Tang et al. [13] investigated five geometric characteristics of the Lining Pump as critical aspects in order to discover the optimal structure of the pump. Entropy generation and flow characteristics for a backward centrifugal fan were explored by Ding et al. [14] examined the influence of a centrifugal fan's blade exit angle on the flow field and pressure changes. Their findings revealed that adjusting the angle has an impact on the fan's performance. Babubhai et al. [15] conducted a study involving three distinct blade geometries of a fan. They performed both experimental and numerical analyses and compared the results. Given the wide-ranging applications of fans, where the performance characteristics of the fan are critical factors, understanding the design of radial fans is of paramount importance. Such knowledge not only enhances operational efficiency but also significantly impacts production costs and energy consumption. In this article, we have employed meticulous computational techniques to simulate and analyze the behavior of a radial fan. The investigation has included variations in critical geometric parameters, providing valuable insights into their direct influence on fan performance. Additionally, the validation of our simulation results through experimental setups underscores the reliability of our findings. By examining these factors collectively, we aim to provide engineers and designers with valuable knowledge to enhance fan designs, ultimately leading to cost-effective, energy-efficient, and high-performance systems.

2 Geometry and physical properties

In this section, an overview of the structural components of the radial fan is provided. Figure (1) offers a visual representation of the fan's geometry, highlighting its two primary constituents: the impeller and the casing. The impeller is comprised of four essential elements, including the disk, blades, shroud, and hub. The disk is situated at the center, and it is attached to the shaft. The blades, characterized by their curved or angled surfaces, are mounted onto the disk and are responsible for generating airflow and pressure, imparting energy to the fluid. Surrounding the blades, the shroud, which serves as the outer part of the impeller, encloses and directs the flow of fluid. In the center of the impeller lies the hub, which is the central portion responsible for transferring torque from the motor to the fluid. Notably, the impeller rotates at a speed of 2968 rpm, a key parameter that significantly influences the fan's performance and its ability to efficiently manipulate airflow and pressure.

The density and dynamic viscosity of the air are 1.045 kg/m^3 and 1.75×10^{-5} kg/m.s, respectively. These fluid properties are fundamental factors governing the behavior of the airflow within the radial fan system. Table (1) provides essential geometric information about the fan, encompassing parameters such as the number of blades, distance between the disk and shroud, blade thickness, air inlet duct diameter, and impeller outer diameter. These geometric details collectively define the fan's physical structure.

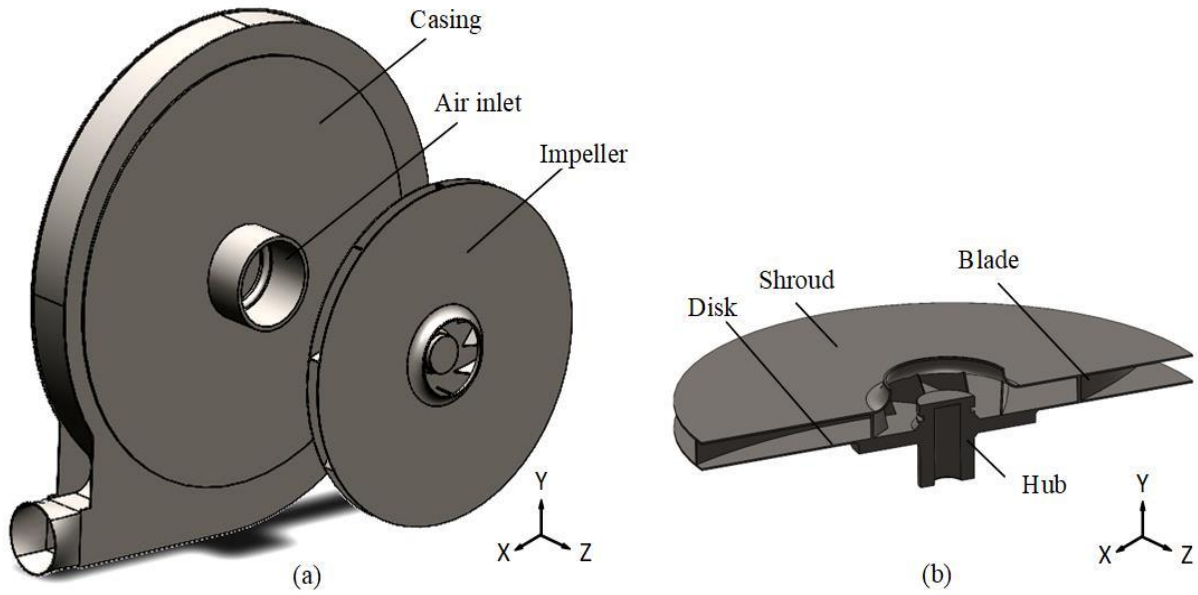

Figure 1 (**a**) Radial fan and (**b**) impeller section view

Table 1 Geometric information

Parameters	Values
Blades number	9
Impeller width	35 mm
Blade thickness	3 mm
Diameter of air inlet duct	200 mm
Impeller outer diameter	800 mm
Outlet angle	64°
Inlet angle	36°

7In this study, an investigation into the impact of altered geometric parameters on the radial fan's performance is conducted. Four critical parameters, as detailed in Table (2), were selected for analysis: the number of blades, impeller width (distance between the disk and shroud), outlet angle, and inlet angle. By altering these geometric parameters, we aimed to elucidate the direct influence of these design variations on critical performance metrics, including total pressure difference, static pressure difference, fan efficiency, and shaft power.

Table 2 Variations in geometric parameters

Parameters	Values
Blades number	9, 11, 13
Impeller width	15 mm, 25 mm, 35 mm
Outlet angle	55°, 64°, 75°
Inlet angle	25°, 36°, 45°

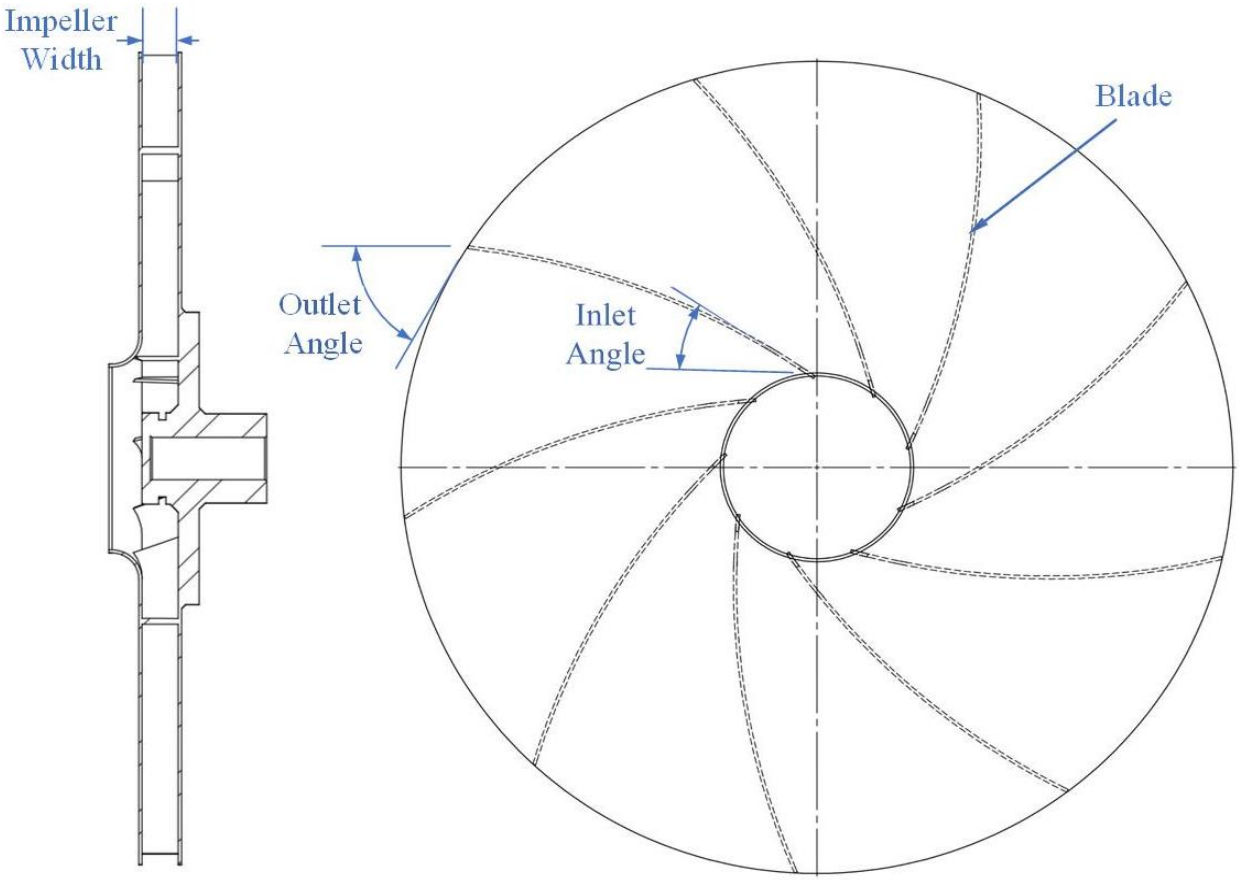

Figure 2 Impeller geometry

Table 3 Geometric variations in simulated configurations

Different geometries	1	2	3	4	5	6	7	8	9
Blades number	9	11	13	9	9	9	9	9	9
Impeller Width	35	35	35	25	15	35	35	35	35
Outlet Angle	64	64	64	64	64	75	55	64	64
Inlet Angle	36	36	36	36	36	36	36	45	25

In total, nine geometries were simulated at various volume flow rates (Table 3). The first geometry served as the base configuration, and for the subsequent geometries, alterations were made to one of the following geometric parameters: Blades number, Impeller Width, Outlet Angle, and Inlet Angle. Figure (2) illustrates the geometric configuration of the impeller, highlighting key parameters such as Blades, Impeller Width, Outlet Angle, and Inlet Angle. These variations allowed for a comprehensive exploration of the impact of different geometries on the simulation results under varying volume flow conditions.

3 Governing equations

The analysis is conducted in three dimensions (3D). Turbulent flow conditions are considered, and the simulation is performed in a steady-state regime. The energy equation is not solved in this context. The governing equations for this study encompass mass and momentum conservation, which are fundamental to understanding the fluid dynamics within the radial fan. These equations are described as follows:

$$\nabla . \overrightarrow{u_r} = 0 \tag{1}$$

Here, ρ denotes the fluid density, and $\vec{u}_r$ represents the relative velocity within the system.

$$\nabla . (\rho \vec{u}_r \, \vec{u}_r) + \rho(\vec{\omega} \times \vec{\omega} \times r + 2\vec{\omega} \times \vec{u}_r \,) = \nabla . \bar{\tau}_r - \nabla p \tag{2}$$

Here, $\vec{\omega}$ represents the angular velocity of the system, r is the radial distance, and $\bar{\tau}_r$ signifies shear stress within the fluid. The terms $\vec{\omega} \times \vec{\omega} \times r$ and $\vec{\omega} \times \vec{u}_r$ correspond to the centrifugal and Coriolis forces, respectively. Furthermore, the realizable $k - \varepsilon$ turbulence model is used to represent turbulent flow in the simulations.
Several essential performance metrics of radial fans are investigated. Equation 3 defines the total pressure difference (ΔP_{total}) as the sum of static pressure difference (ΔP_{static}) and dynamic pressure difference ($\Delta P_{dynamic}$). Equation 4 provides insight into the power requirement of the fan, denoted as P_{shaft}, where torque (T) is multiplied by angular velocity (ω). Equation 5 shows the fan's efficiency (η), which relates the total pressure difference (ΔP_{total}) and volumetric flow rate (Q) to the shaft power (P_{shaft}).

$$\Delta P_{total} = \Delta P_{static} + \Delta P_{dynamic} \tag{3}$$

$$P_{shaft}(\mathrm{W}) = T(\mathrm{N.m}) \times \omega \left(\frac{\mathrm{rad}}{\mathrm{s}}\right) \tag{4}$$

$$\eta = \frac{\Delta P_{total}(\mathrm{pa}) \times \; Q\left(\frac{\mathrm{m}^3}{\mathrm{s}}\right)}{T(\mathrm{N.m}) \times \omega \left(\frac{\mathrm{rad}}{\mathrm{s}}\right)} \tag{5}$$

4 Solution method and boundary conditions

In order to ensure accurate analysis, a computational approach was employed using commercial software. A detailed model of the radial fan was created in SolidWorks to represent the fan's physical structure. Subsequently, the fan geometry was meshed using ANSYS meshing tools, creating a grid for numerical calculations. The Finite-Volume Method was chosen as the numerical framework for the analysis. The simulations were conducted using ANSYS Fluent.

Notably, the Moving Reference Frame (MRF) method was utilized. This technique involved defining a special zone around the rotating part of the fan, which expedited simulations without compromising accuracy. Boundary conditions were applied to define how the fan interacts with its environment in the virtual model. An inlet condition was set to represent the volume of air the fan intakes (mass flow rate), while the outlet condition reflected the pressure at the fan's outlet. Additionally, wall conditions were applied to the fan's surfaces, accounting for the no-slip behavior of air at these surfaces.

5 Numerical simulation and grid independence

To ensure the reliability of the computational analysis, a grid independence study has been conducted. Two distinct meshing methods were employed, one with and another without the cut cell approach. In the cut cell method, the largest cell dimension is a multiple of the smallest cell size raised to a power of two [16]. This approach aimed to enhance grid quality, as evidenced by the achieved skewness close to zero and orthogonality close to one, coupled with a reduction in the overall number of elements. Figure (2) provides a sectional view of this grid configuration.

For the grid independence study, as illustrated in Figure (3), we increased the number of mesh elements while measuring the total pressure difference between the fan's inlet and outlet. After reaching a count of 2,950,000 elements, minimal variations were observed in the total pressure difference. Consequently, we concluded that a mesh configuration comprising 2,950,000 elements sufficed to ensure grid independence and reliable results for our analysis.

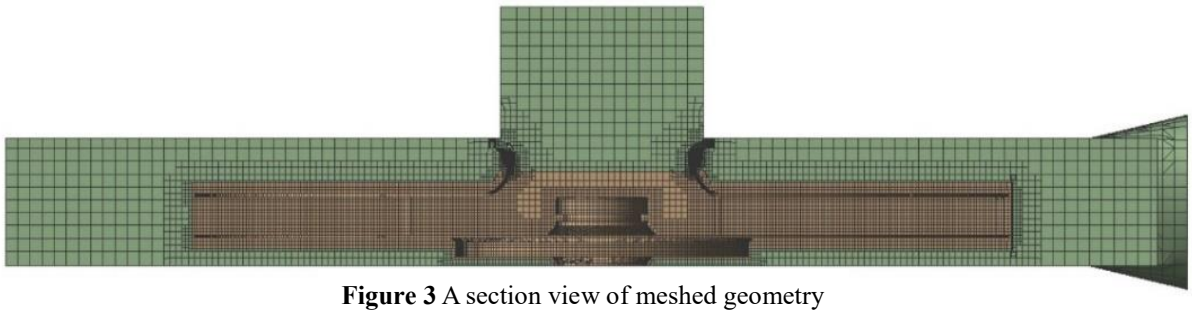

Figure 3 A section view of meshed geometry

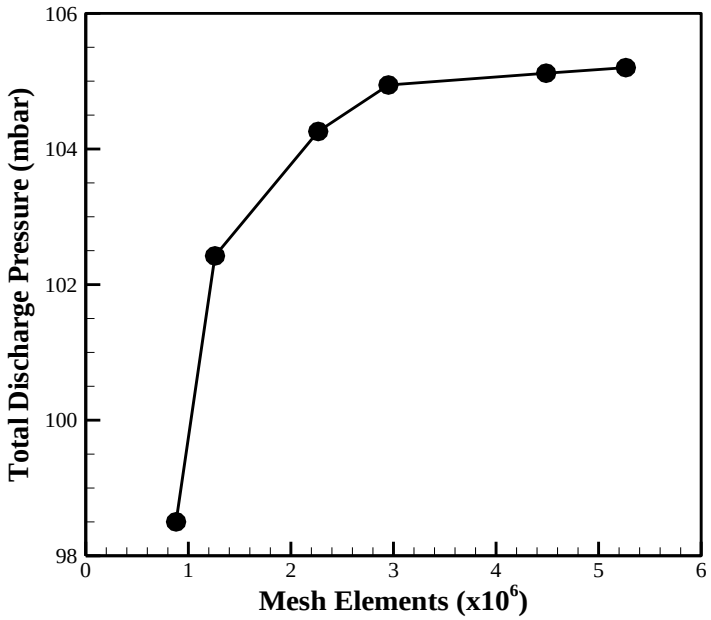

Figure 4 Mesh independence study

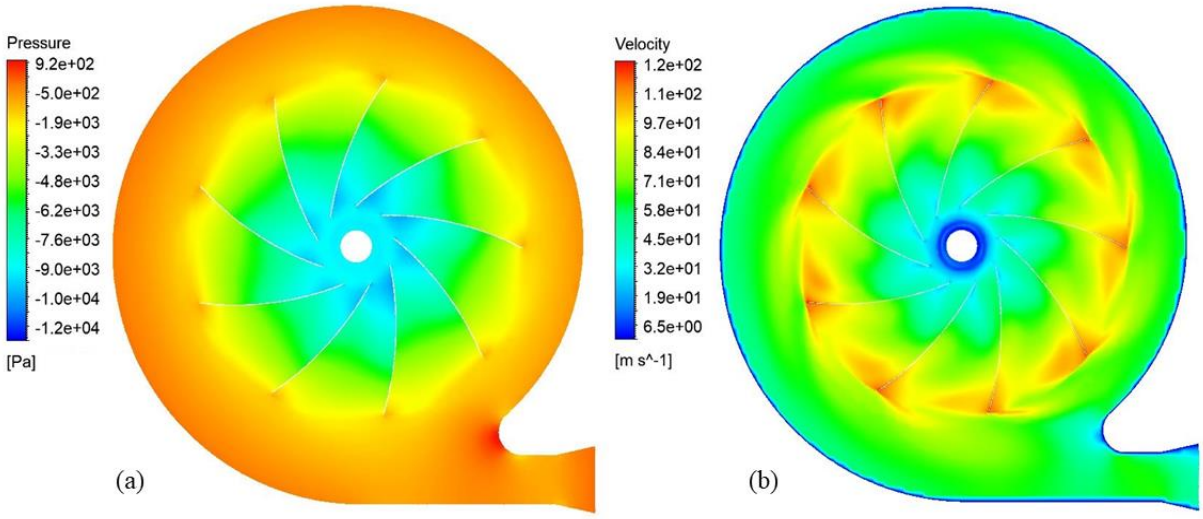

Figure 5 Contours in the first plane at a volumetric flow rate of 2991 m³/hr: **a**) total Pressure, and **b**) velocity

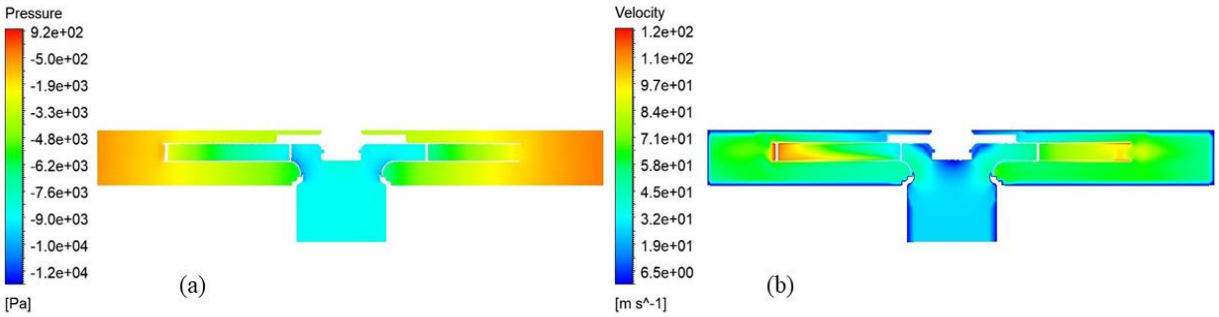

Figure 6 Contours in the second plane at a volumetric flow rate of 2991 m³/hr: **a**) total Pressure, and **b**) velocity

Figures (4) and (5) present the contours at a volumetric flow rate of 2991 m^3/hr, representing the maximum pressure output achievable by the fan. In Figure (4), the contours of total pressure and velocity are shown on a plane that is created by crossing the x and y axes and going through the center of the impeller. A second plane formed by crossing the x and z axes and going through the impeller's center is shown in Figure (5) as total pressure and velocity contours. According to the pressure contour, low-pressure air enters the fan and increases as it moves through the blades. In addition, the fluid enters the impeller at a low velocity before increasing as it approaches the blades' ends.

6 Validation

The validation of our computational results involved a comparison with our experimental data to ensure the accuracy of our simulations. Figure (6) provides a visual representation of the experimental setup employed for this validation process. To assess the alignment between our numerical and experimental findings, we examined Figure (7). This figure illustrates the comparison of total pressure differences and static pressure differences between the fan's inlet and outlet across a wide range of volumetric flow rates (678, 1132, 1475, 1746, 1976, 2205, 2313, 2579, 2647, 2839, and 2991 cubic meters per hour). When operating at a flow rate of 1475 cubic meters per hour, we observed the most substantial static and total pressure differences. Our analysis revealed that the maximum error between the experimental and numerical results was 3%, occurring at the 2205 cubic meters per hour flow rate. This level of accuracy highlights the good agreement between our numerical simulations and the experimental data, validating the reliability of our computational approach.

Figure 7 The experimental setup

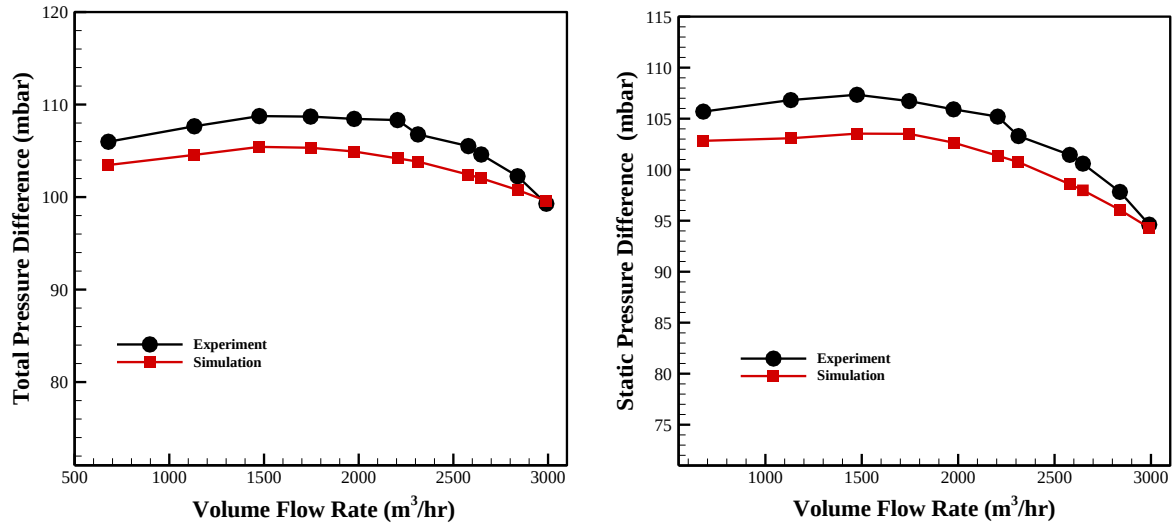

Figure 8 Comparison of total and static pressure differences between inlet and outlet with experimental results

The pressure readings maintained a deviation of no more than ± 0.2% from the actual values, while temperature assessments were equally precise, boasting a reliability margin within ± 0.2% of the measured values. Voltage assessment tools had a ± 1% precision, while current evaluation tools showcased a ± 1.5% precision. The empirically measured shaft power, under the assumption of a cosφ value of 0.9, involved experimentation to acquire voltage (V) and current (I) in accordance with the equation $P = \sqrt{3}VIcos\varphi$.

7 Results

This section provides an analysis of the radial fan's performance, utilizing four sets of graphs. Each set of graphs investigates the influence of a geometric parameter on the fan's performance.

In Figure (8), we explore the impact of varying blade counts, while Figure (9) considers changes in impeller width. Figure (10) shifts the focus to impeller inlet angles, and Figure (11) examines impeller outlet angles. For each of these four geometric parameters, we explore three different values. Within each figure, we present four plots, detailing critical performance metrics, including total pressure difference, static pressure difference, shaft power, and efficiency. These parameters are of importance in assessing fan performance and are assessed across different volume flow rates.

Figure (8) presents a comparison of the radial fan's performance across three different blade configurations: 9 blades, 11 blades, and 13 blades. The figure features four distinct plots, each focusing on essential performance metrics. In the total pressure difference and static pressure difference plots, it's clear that an increase in the number of blades results in higher static and total pressure differences. The fan with 11 blades exhibits the lowest efficiency among the three configurations, while both the 9 and 13 blade configurations display higher efficiency. In the plot for shaft power, we observe that the fan equipped with 11 blades has the highest shaft power, surpassing the power output of both 9 and 13 blade configurations.

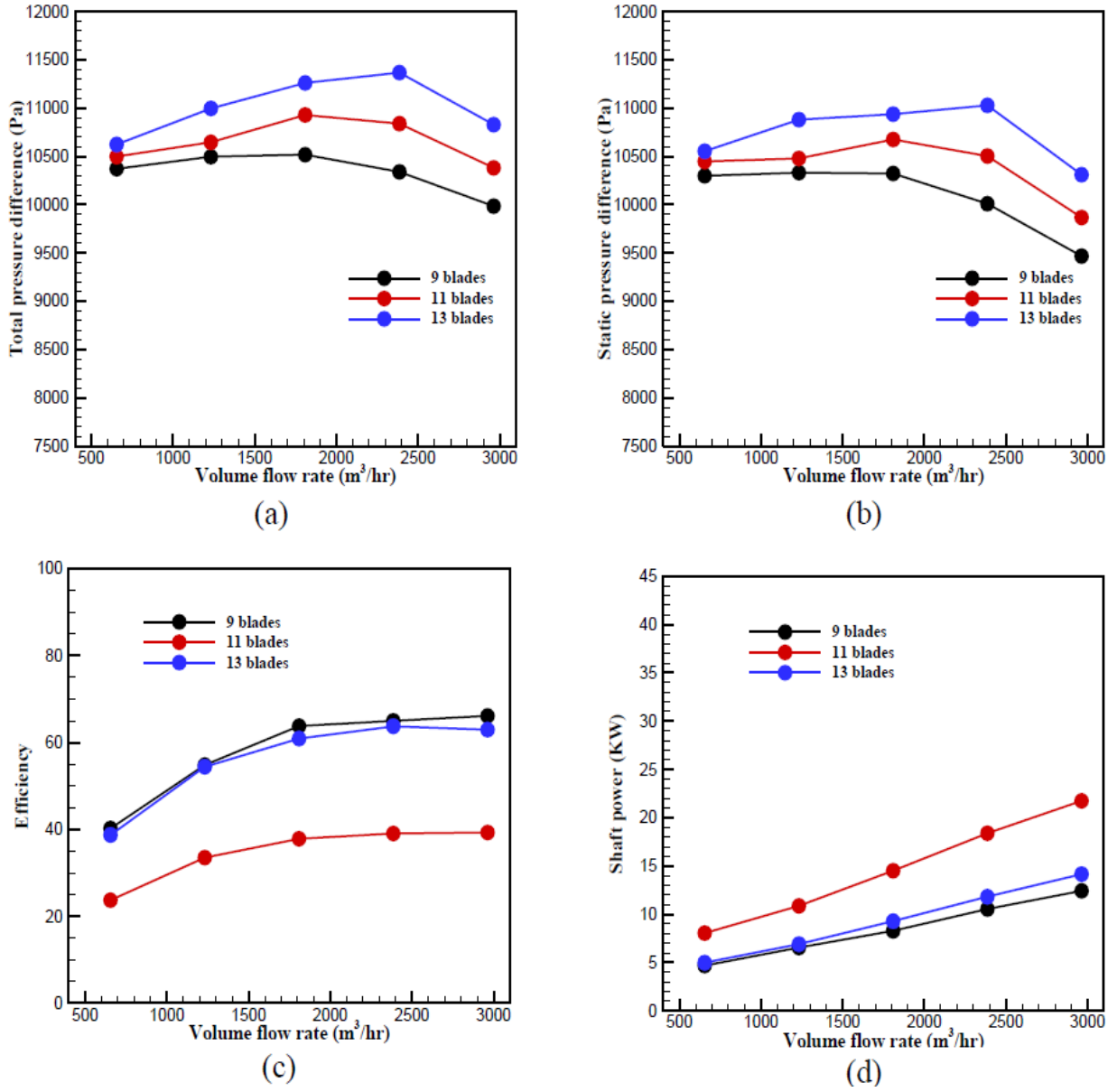

Figure 9 Comparing radial fan performance for different blades: **a**) total pressure difference, **b**) static pressure difference, **c**) efficiency, and **d**) shaft power

In Figure (9), the impact of different impeller widths on the radial fan's performance is explored. Examining the static and total pressure difference plots reveals a consistent trend of increasing in impeller width corresponds to higher total and static pressure differences. The efficiency plot highlights that an impeller width of 25 exhibits the lowest efficiency compared to the other widths. Also, while an impeller width of 15 provides the highest efficiency up to 1800 cubic meters per hour, width 35 exhibits the highest efficiency for larger flow rates. The shaft power plot shows that width 15 has the lowest shaft power, while width 25 has the highest.
Figure (10) presents an examination of our radial fan's performance under varying blade inlet angles, focusing on total pressure difference, static pressure difference, shaft power, and efficiency. The analysis reveals that altering the blade inlet angles has minimal impact on total and static pressure differences as well as shaft power. However, the efficiency plot indicates that selecting a blade inlet angle of 25 degrees leads to decreased efficiency compared to other angles. However, as the flow rate increases, the influence becomes negligible.

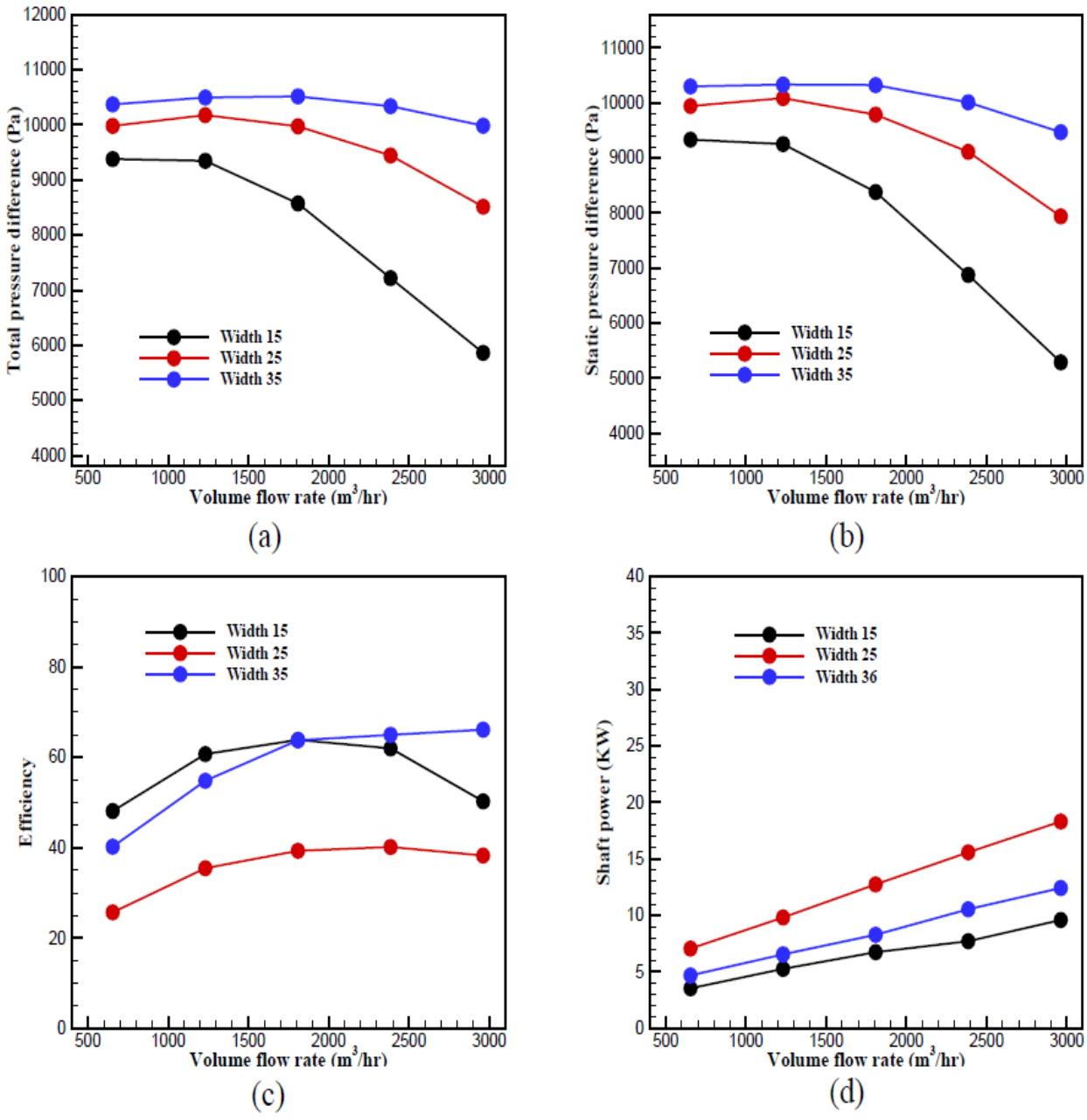

Figure 10 Comparing radial fan performance for different impeller widths: **a**) total pressure difference, **b**) static pressure difference, **c**) efficiency, and **d**) shaft power.

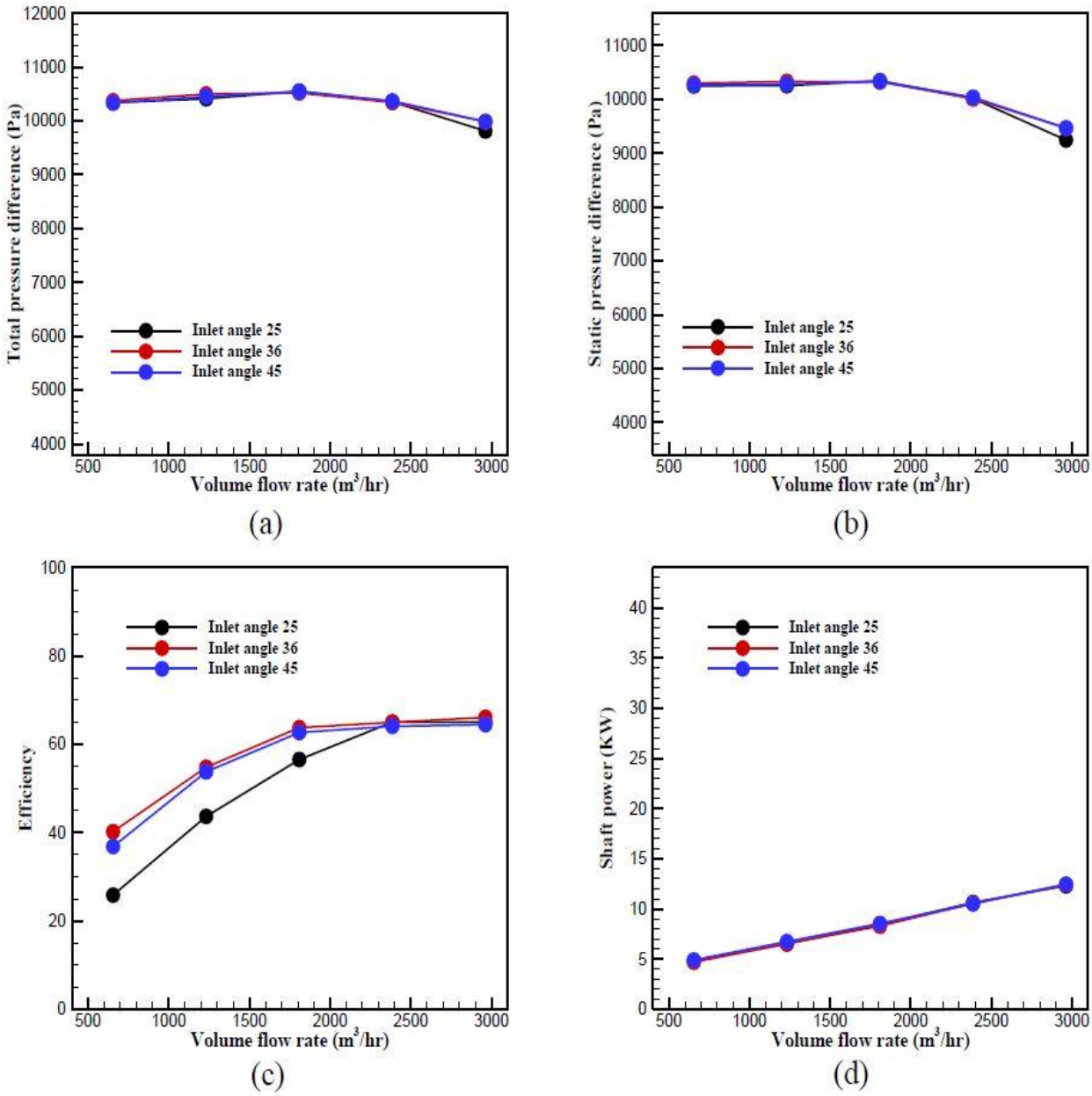

Figure 11 Comparing radial fan performance for different impeller inlet angles: **a**) total pressure difference, **b**) static pressure difference, **c**) efficiency, and d) shaft power.

Figure (11) explores how different outlet angles affect the radial fan's performance. Across the four plots within the figure, it is notable that the results for an outlet angle of 55 degrees exhibit greater variance compared to those for angles 64 and 75 degrees. The results for outlet angles 64 and 75 degrees are closely aligned. Outlet angle 55 degrees stands out by displaying lower static and total pressure compared to the other two angles. Additionally, its efficiency is lower, particularly evident at volume flow rates below 2500 m³/hr. Furthermore, when examining shaft power, it's apparent that outlet angle 55 degrees yields higher power output at lower volume flow rates.

Tables (2), (3), (4), and (5) exhibit a comprehensive investigation into the influence of diverse geometric parameters on total pressure difference, static pressure difference, overall efficiency, and shaft power, respectively. Each table categorizes data based on varied volume flow rates and specific geometric configurations such as the number of blades, width, inlet angle, and outlet angle. The application of a color-coded scale, where blue denotes higher values and red represents lower values, facilitates a rapid visual assessment of relative magnitudes across different scenarios.

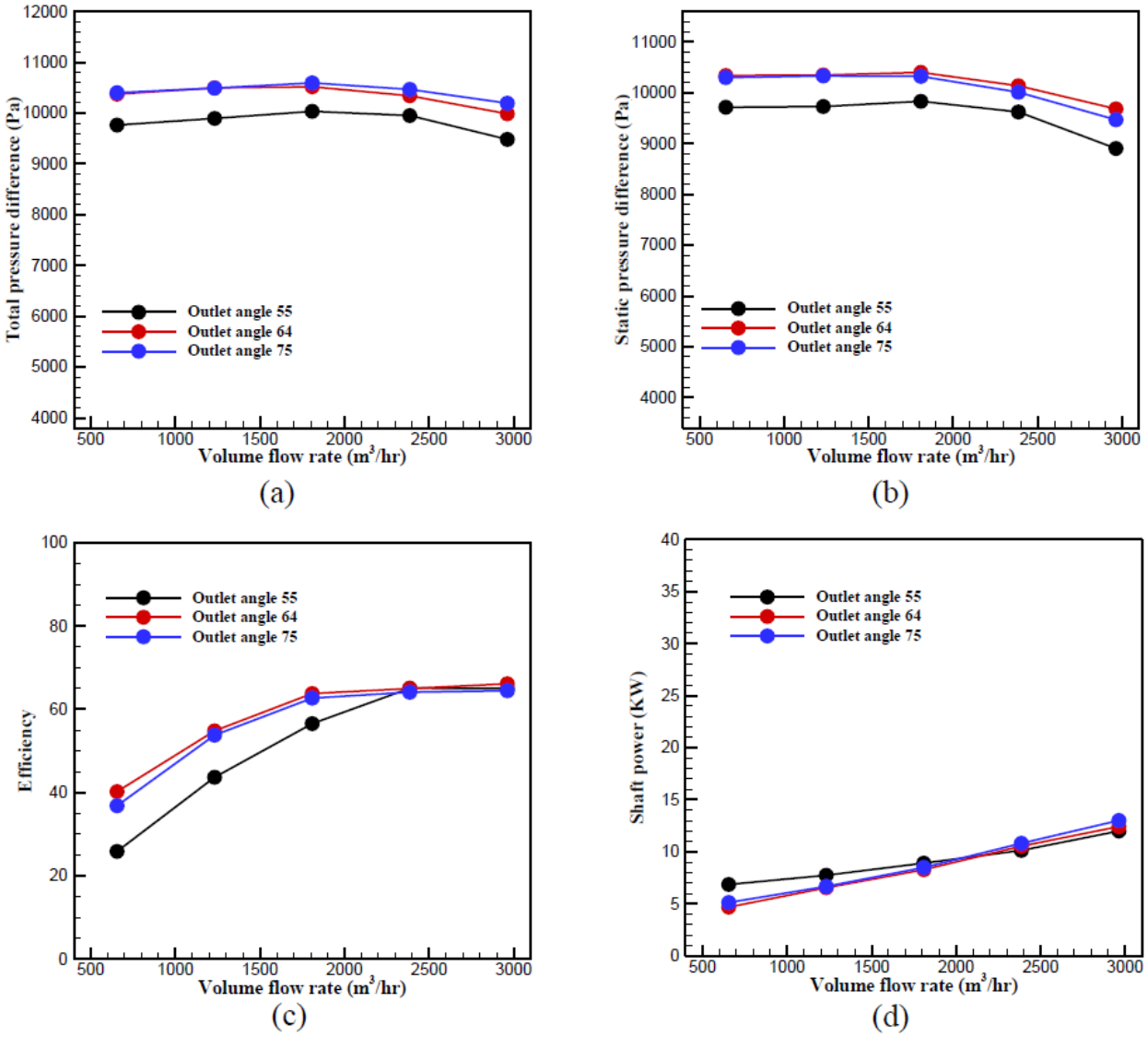

Figure 12 Comparing radial fan performance for different impeller outlet angles: **a**) total pressure difference, **b**) static pressure difference, **c**) efficiency, and **d**) shaft power

Table 4 Influence of geometric parameters on total pressure difference

Volume flow rate (m^3/hr)	655	1232	1809	2386	2963
9 blades	10372.1	10497.6	10517.9	10340.1	9985.2
11 blades	10499.2	10646.6	10929.4	10839.2	10381.7
13 blades	10623.7	10997.3	11261.4	11367.6	10829.0
Width: 15 mm	9380.2	9347.8	8575.1	7219.1	5861.2
Width: 25 mm	9981.8	10177.2	9974.3	9445.5	8514.7
Width: 35 mm	10372.1	10497.6	10517.9	10340.1	9985.2
Inlet Angle: 25°	10340.3	10408.8	10551.9	10351.2	9810.4
Inlet Angle: 36°	10372.1	10497.6	10517.9	10340.1	9985.2
Inlet Angle: 45°	10331.5	10453.1	10540.8	10369.3	9985.6
Outlet Angle: 55°	9763.5	9894.8	10034.1	9950.8	9481.8
Outlet Angle: 64°	10372.1	10497.6	10517.9	10340.1	9985.2
Outlet Angle: 75°	10401.3	10490.0	10593.6	10466.1	10194.2

Table 5 Influence of geometric parameters on static pressure difference

Volume flow rate (m^3/hr)	655	1232	1809	2386	2963
9 blades	10299.0	10331.4	10323.2	10010.2	9467.8
11 blades	10448.1	10479.3	10675.3	10503.8	9867.6
13 blades	10554.0	10880.9	10937.5	11029.1	10311.0
Width: 15 mm	9332.5	9251.8	8381.4	6877.3	5291.7
Width: 25 mm	9942.0	10087.0	9787.4	9111.5	7939.8
Width: 35 mm	10299.0	10331.4	10323.2	10010.2	9467.8
Inlet angle: 25°	10248.7	10251.3	10345.1	10013.8	9242.9
Inlet angle: 36°	10299.0	10331.4	10323.2	10010.2	9467.8
Inlet angle: 45°	10270.2	10282.8	10330.3	10037.7	9463.4
Outlet angle: 55°	9715.0	9728.3	9830.9	9621.9	8902.6
Outlet angle: 64°	10299.0	10331.4	10323.2	10010.2	9467.8
Outlet angle: 75°	10339.5	10350.0	10401.1	10137.0	9682.1

Table 6 Influence of geometric parameters on efficiency

Volume flow rate (m^3/hr)	655	1232	1809	2386	2963
9 blades	40.2	54.8	63.8	65.0	66.1
11 blades	23.7	33.5	37.8	39.1	39.3
13 blades	38.7	54.4	60.9	63.7	63.0
Width: 15 mm	48.1	60.7	63.9	62.0	50.3
Width: 25 mm	25.7	35.4	39.3	40.1	38.3
Width: 35 mm	40.2	54.8	63.8	65.0	66.1
Inlet angle: 25°	39.3	54.7	62.8	64.5	65.7
Inlet angle: 36°	40.2	54.8	63.8	65.0	66.1
Inlet angle: 45°	38.3	53.1	62.0	65.4	66.0
Outlet angle: 55°	25.9	43.7	56.5	65.0	65.0
Outlet angle: 64°	40.2	54.8	63.8	65.0	66.1
Outlet angle: 75°	36.8	53.8	62.7	64.1	64.5

Table 7 Influence of geometric parameters on shaft power

Volume flow rate (m^3/hr)	655	1232	1809	2386	2963
9 blades	4.69	6.55	8.29	10.55	12.43
11 blades	8.05	10.87	14.51	18.39	21.75
13 blades	4.99	6.92	9.29	11.82	14.16
Width: 15 mm	3.55	5.27	6.75	7.72	9.60
Width: 25 mm	7.07	9.82	12.75	15.59	18.32
Width: 35 mm	4.69	6.55	8.29	10.55	12.43
Inlet angle: 25°	4.79	6.51	8.45	10.64	12.30
Inlet angle: 36°	4.69	6.55	8.29	10.55	12.43
Inlet angle: 45°	4.90	6.73	8.54	10.51	12.45
Outlet angle: 55°	6.86	7.75	8.92	10.14	12.00
Outlet angle: 64°	4.69	6.55	8.29	10.55	12.43
Outlet angle: 75°	5.13	6.67	8.49	10.82	13.02

8 Conclusions

In conclusion, this study explored how different design aspects impact the performance of a radial fan. By comparing computer simulations with real-world experiments, we found that our simulations closely matched the actual performance, with only a 3% difference at most. We looked at four key design factors: the number of blades, impeller width, blade outlet angle, and blade inlet angle. Here's what we discovered:

- The number of blades influenced static and total pressure differences. Fans with 11 blades were less efficient than those with 9 or 13 blades.
- Impeller width affected static and total pressure differences. A width of 25 mm resulted in lower efficiency.
- Blade inlet angle had minimal impact on most performance metrics, except for efficiency, which decreased at a 25-degree angle.
- Outlet angle variations affected fan performance, with a 55-degree angle showing distinct characteristics like lower pressure differences and efficiency, especially at lower airflow rates.

Overall, the research findings suggest that optimal performance can be achieved with a certain geometric configuration, and those design parameters shift with flow rate. Consequently, this study provides valuable insights for engineers and designers aiming to optimize fan efficiency and reliability. It also highlights the importance of computational simulations in making informed decisions about fan design and operation.

References

[1] A. Behzadmehr and Y. Mercadier, "Numerical Study of Flow Parameters and Entropy Generation on a Centrifugal Fan," International Journal of Exergy, Vol. 6, No. 1, pp. 80-92, 2009, doi: https://doi.org/10.1504/IJEX.2009.023346.

[2] Y. J. Kim, "Flow Characteristics in a Cross-flow Fan with Various Design Parameters," in *Fluid Machinery and Fluid Mechanics: 4th International Symposium (4th ISFMFE)*, 2009: Springer, Berlin, Heidelberg., pp. 255-261, doi: https://doi.org/10.1007/978-3-540-89749-1_38.

[3] J. Feng, F.-K. Benra, and H. Dohmen, "Application of Different Turbulence Models in Unsteady Flow Simulations of a Radial Diffuser Pump," *Forschung im Ingenieurwesen*, Vol. 3, No. 74, pp. 123-133, 2010, doi: https://doi.org/10.1007/s10010-010-0121-4.

[4] Y. Gui and P. Xi, "Study on the Methods of Determining Main Geometric Parameters of Centrifugal Fan Impeller," in *2010 The 2nd International Conference on Computer and Automation Engineering (ICCAE)*, 2010, IEEE, Singapore, Vol. 4, pp. 42-46, doi: https://doi.org/10.1109/ICCAE.2010.5451790.

[5] L. Chunxi, W. S. Ling, and J. Yakui, "The Performance of a Centrifugal Fan with Enlarged Impeller," *Energy Conversion and Management*, Vol. 52, No. 8-9, pp. 2902-2910, 2011, doi: https://doi.org/10.1016/j.enconman.2011.02.026.

[6] B. Jafarzadeh, A. Hajari, M. Alishahi, and M. Akbari, "The Flow Simulation of a Low-specific-speed High-speed Centrifugal Pump," *Applied Mathematical Modelling*, Vol. 35, No. 1, pp. 242-249, 2011, doi: https://doi.org/10.1016/j.apm.2010.05.021.

[7] O. Singh, T. Sreenivasulu, and M. Kannan, "Influence of Geometric Parameters on Centrifugal Fan Performance and its Significance in Automotive Applications," *International Journal of Modeling, Simulation, and Scientific Computing,* Vol. 3, No. 03, p. 1250007, 2012, doi: https://doi.org/10.1142/S1793962312500079.

[8] O. Petit and H. Nilsson, "Numerical Investigations of Unsteady Flow in a Centrifugal Pump with a Vaned Diffuser," *International Journal of Rotating Machinery,* Vol. 2013, 2013, doi: https://doi.org/10.1155/2013/961580.

[9] H. Ratter, Ş. Çağlar, and M. Gabi, "A Coupled Blade Adjustment and Response Surface Method for the Optimization of Radial Fans without Housing,"In *Turbo Expo: Power for Land, Sea, and Air,* 2014, Vol. 45578: American Society of Mechanical Engineers, p. V01AT10A009, doi: https://doi.org/10.1115/GT2014-25564.

[10] K. Sun, H. Ouyang, J. Tian, Y. Wu, and Z. Du, "Experimental and Numerical Investigations on the Eccentric Vortex of the Cross Flow Fan," *International Journal of Refrigeration,* Vol. 50, pp. 146-155, 2015, doi: https://doi.org/10.1016/j.ijrefrig.2014.10.005.

[11] N. Rajabi, R. Rafee, and S. Farzam-Alipour, "Effect of Blade Design Parameters on Air Flow through an Axial Fan," *International Journal of Engineering,* Vol. 30, No. 10, pp. 1583-1591, 2017, doi: https://doi.org/10.5829/ije.2017.30.10a.20.

[12] S. Huang, Y. Wei, C. Guo, and W. Kang, "Numerical Simulation and Performance Prediction of Centrifugal Pump's Full Flow Field Based on OpenFOAM," *Processes,* Vol. 7, No. 9, p. 605, 2019, doi: https://doi.org/10.3390/pr7090605.

[13] L. Tang, M. Liu, and F. Ma, "Thermosetting Coupling Analysis and Parameter Optimization of the Plastic Lining Pump Structure," *Advances in Materials Science and Engineering,* Vol. 2019, 2019, doi: https://doi.org/10.1155/2019/3790167.

[14] H. Ding, T. Chang, and F. Lin, "The Influence of the Blade Outlet Angle on the Flow Field and Pressure Pulsation in a Centrifugal Fan," *Processes,* Vol. 8, No. 11, p. 1422, 2020, doi: https://doi.org/10.3390/pr8111422.

[15] V. K. P. Babubhai, A. Chaudhari, A. Sharma, and V. Diwakar, "Experimental and Numerical Study on the Influence of Flow Passages in Centrifugal Fan using Computational Fluid Dynamics," *Engineering Research Express,* Vol. 5, No. 2, p. 025030, 2023, doi: https://doi.org/10.1088/2631-8695/accf00.

[16] T. Canonsburg, "Ansys Meshing User's Guide," Vol. 15317, pp. 724-746, 2013, https://dl.cfdexperts.net/cfd_resources/Ansys_Documentation/Ansys_Meshing/Ansys_Meshing_Users_Guide.pdf.